Int. J. Heat Mass Transfer. Vol. 33, No. 1, pp. 9–18, 1990
Printed in Great Britain

0017-9310/90 $3.00 + 0.00

Convective mass transfer from a square cylinder and its base plate

R. J. GOLDSTEIN,† S. Y. YOO‡ and M. K. CHUNG§

†Department of Mechanical Engineering, University of Minnesota, Minneapolis, MN 55455, U.S.A.
‡Department of Mechanics and Design, Chungnam National University, Daejeon, Korea
§Department of Mechanical Engineering, Korea Advanced Institute of Science and Technology, Seoul, Korea

(*Received* 4 *August* 1988 *and in final form* 31 *March* 1989)

Abstract—The mass transfer from a square cylinder and from the plate on which the cylinder is mounted vertically, is investigated with the naphthalene sublimation technique. The general pattern of local mass transfer is somewhat different from that with a circular cylinder. A comparison with heat transfer measurements on a square cylinder in the two-dimensional flow region, using the heat/mass transfer analogy, shows good agreement in average transfer rates, but slight differences in local values. A dramatic change of mass transfer rates is found both on the cylinder and the base plate around the plate–cylinder junction region due to a horseshoe vortex system. Multiple vortices, which include the primary horseshoe vortex, the corner vortex and two pairs of counterrotating vortices, affect the mass transfer process. Variation of either Reynolds number or initial boundary layer thickness does not significantly change the location of the peaks created by the horseshoe vortex system, but only affects the magnitude of the local mass transfer rate. Visualization of the surface flow on the base plate is included to supplement the mass transfer measurements.

INTRODUCTION

NUMEROUS investigations, both theoretical and experimental, have been conducted on the heat or mass transfer from a circular cylinder in crossflow in the two-dimensional flow region. Relatively little attention has been given to a square/rectangular cylinder because of the complexity of the flow pattern and the difficulty in measurement. Reiher [1] and Hilpert [2] reported average heat transfer rates from a square cylinder. Recently Igarashi [3–5] performed a series of experiments investigating fluid flow and heat transfer around a square/rectangular cylinder. He measured local and average heat transfer rates on a square cylinder at various angles of attack and on a rectangular cylinder at various width-to-height ratios. He then correlated heat transfer coefficients with flow characteristics. The first purpose of the present study is to measure local mass transfer rates on a square cylinder in the two-dimensional flow region. A naphthalene sublimation technique is employed. Only the middle portion of the cylinder, far from the base plate, is coated with naphthalene. A comparison with Igarashi's [4] heat transfer measurements is made to examine the heat/mass transfer analogy for this flow.

A basic understanding of the characteristics of fluid flow and heat transfer around an obstacle protruding from a flat plate is very important for the successful design of compact heat exchangers, turbine blades, air foils, electronic chips, and many other structures. Nevertheless, little information is presently available about such complicated, three-dimensional separated flows. It is well known that a horseshoe vortex system is the dominant flow phenomena in the plate–obstacle junction region. By using smoke and oil flow visualization and by measuring the surface pressure distribution, Baker [6] found multiple vortices formed around the base of a circular cylinder. He investigated the variation of the horseshoe vortex system and the boundary layer separation point with the flow parameters. Surface flow visualization and surface static pressure measurements as well as mean velocity and pressure measurements in and around the vortex system have been presented by Eckerle and Langston [7]. Contrary to Baker [6], they found only a single primary vortex. Several investigators have studied the influence of the horseshoe vortex system on the heat or mass transfer. Eibeck and Eaton [8] studied the heat transfer effects of an isolated longitudinal vortex embedded in a turbulent boundary layer. They used a vortex generator, and measured surface temperature with thermocouples and the mean velocity distribution using a four hole pressure probe. Graziani *et al.* [9] measured local heat transfer rates with thermocouples on the endwall, and on the suction and pressure surfaces of a large-scale turbine blade, and inquired into the influence of the passage secondary flows on the heat transfer. To examine the enhancement of heat transfer by the leading-edge horseshoe vortex, heat transfer measurements using an infra-red camera were made by Blair [10] on the base plate near the leading edge of a rectangular block. Ireland and Jones [11] measured local heat transfer coefficients both on a circular cylinder and on its base plate using thermochromic liquid crystals.

The vortices created by the three-dimensional

NOMENCLATURE

d	side length of square cylinder, 25.4 mm in the present study
D	mass diffusion coefficient of naphthalene vapor in air
h_m	mass transfer coefficient
H	shape factor, δ_1/δ_2
n	exponent in the heat/mass transfer analogy equation, 1/3 in the present study
Nu	Nusselt number
p	circumferential distance measured from the front-left edge of the cylinder counterclockwise
Pr	Prandtl number
Re_d	Reynolds number, $U_\infty d/\nu$
Sc	Schmidt number, ν/D, approximately 2.0–2.1 in the present tests
Sh	Sherwood number, $h_m d/D$
Δt	net sublimation depth of naphthalene in the wind tunnel
U_∞	freestream velocity, 8.7–17.9 m s^{-1} in the present study
x	streamwise distance measured from the center of the cylinder base
y	distance along the cylinder axis measured from the base
z	spanwise distance measured from the center of the cylinder base.

Greek symbols

δ_1	displacement thickness
δ_2	momentum thickness
ν	kinematic viscosity of air
ρ_s	density of solid naphthalene
$\rho_{v,w}$	naphthalene vapor density on the surface
$\Delta\tau$	total exposure time in the wind tunnel.

secondary flow are so small in size that it is very difficult to detect their existence by conventional methods of measurement. One alternative is to conduct mass transfer experiments. The naphthalene sublimation technique was employed in ref. [12] to investigate circumferential and longitudinal variations of mass transfer rates from a smooth circular cylinder. It was found that a small but very intense vortex produces extremely high mass transfer rates in the front face of a cylinder near the base. The effects of the horseshoe vortex system on the mass transfer from a surface in the region of the base of a protruding circular cylinder was studied in ref. [13]. High enhancement of mass transfer was observed immediately in front, along the side and downstream of the cylinder. Dresar and Mayle [14] also obtained mass transfer data at the base of a circular cylinder both with and without mass transfer from the base plate.

The second purpose of this study is to investigate the nature of the horseshoe vortex system formed around a protruding square cylinder, and how it affects the mass transfer process both on the cylinder and on its base plate. A square cylinder, coated on the bottom portion with naphthalene, is mounted vertically on the base plate that also has an active naphthalene surface. The assembled testpiece is installed in a wind tunnel for about 1 h. Elevation profiles of the naphthalene surface are measured both before and after the test run to determine mass transfer rates. A computer controlled measurement system is used for precise positioning of the sensor and accurate elevation reading. Effects of the Reynolds number and the initial boundary layer thickness (controlled by a tripping wire) on the horseshoe vortex system are also examined. The surface flow on the base plate is visualized with the oil–lampblack technique in order to supplement the mass transfer measurements.

EXPERIMENTAL APPARATUS AND PROCEDURE

Experimental apparatus

An open-circuit suction-type wind tunnel is used for this study. Air, drawn at room temperature, passes through filters, honeycombs, damping screens, and a 9:1 contraction section. This is followed by a 610 mm wide × 305 mm high rectangular test section. The boundary layer on the tunnel's bottom wall is tripped with a circular rod at the beginning of the test section. The displacement thickness and the shape factors of the turbulent boundary layer on the bottom wall at 473 mm downstream from the tripping wires of different size are shown in Table 1. Air speed varies from nominally 8.7 to 17.9 m s^{-1} corresponding to Re_d, the Reynolds number based on the length of a side of the square cylinder, from 13 600 to 28 000. The freestream turbulence intensity is less than 0.6% over the entire range of speeds. Freestream velocity is determined using an impact tube in conjunction with a wall static tap. Boundary layer profiles are measured without the test cylinder installed to determine the boundary layer thickness.

Figure 1 shows two test cylinders made of aluminum. Also shown is the mounting plate. A derlin plate is used for the two-dimensional measurements, while an aluminum plate is used for the three-dimensional

Table 1. Boundary layer parameters on the bottom plate of the wind tunnel for different tripping wires (located at $x/d = -18.6$)

d_{trip}(mm)	Re_d	δ_1(mm)	H
1.65	18 800	2.475	1.396
6.35	18 400	4.152	1.292
12.7	18 800	6.586	1.254

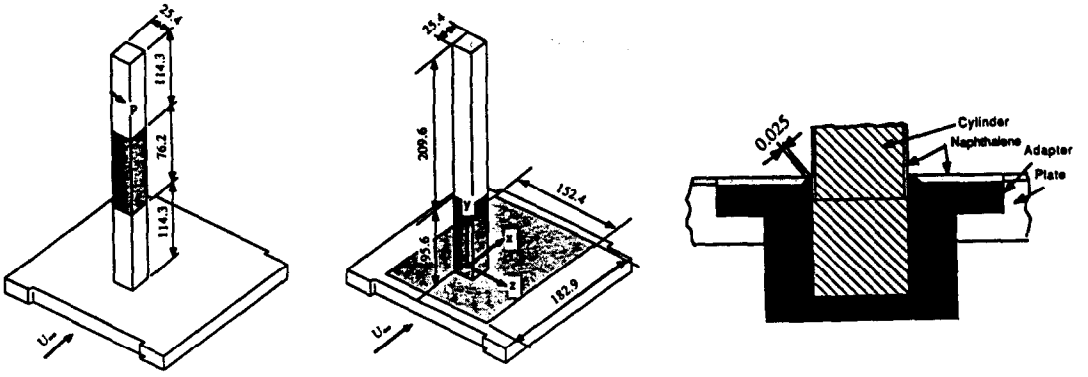

(a) (b) (c)

FIG. 1. Sketch of square cylinders and base plate for mass transfer measurements (units in mm; shaded area represents naphthalene surface): (a) testpiece for measurements in two-dimensional flow region; (b) testpiece for measurements near and on base plate; (c) details near the plate–cylinder junction of (b).

measurements. The cylinder used for the two-dimensional measurements, is machined with a 1 mm deep and 76.2 mm long section in the outer middle surface to hold the cast naphthalene. It is mounted on the derlin plate that has the same configuration as the hole of the tunnel's bottom wall. For three-dimensional measurements, the naphthalene section on the cylinder is machined into the outer bottom surface. This cylinder is inserted into a removable adapter of the base plate so that the naphthalene covered portion extends from 6 mm below the upper surface of the plate to 95.6 mm above it. The base plate has a 152.4 mm × 182.9 mm by 1.5 mm deep naphthalene active region. The upper surface of the plate is aligned flush with the bottom wall of the wind tunnel. The test cylinder is positioned vertically in the middle of the tunnel's cross-section, approximately 473 mm downstream of the boundary layer trip. To monitor the naphthalene surface temperature during a test run, 0.25 mm copper–constantan thermocouples are installed at several locations in the naphthalene on the cylinder and the base plate.

The automated data acquisition system used to measure local sublimation depth consists of a depth gauge with a signal conditioner, a digital multimeter, two stepper motors, a motor control unit, and an HP-85 microcomputer. A Schaevitz Linear Variable Differential Transformer (LVDT) gauge, having a 0.5 mm operational range and 2.54×10^{-5} mm (1×10^{-6} in.) resolution, is connected to a Schaevitz CAS-025 signal conditioner. A digital multimeter acquires the signal from the signal conditioner and sends it to the HP-85 microcomputer. Then the HP-85 transfers the signal to an IBM-XT for data reduction and storage. The HP-85 and the motor control unit control the stepper motors used to position the LVDT sensor. The stepper motors are able to move the sensor in 0.0254 mm (0.001 in.) increments.

Procedure

A new naphthalene casting is made for each test run. The square cylinder is clamped within a four-piece aluminum mold and the test plate is clamped to a highly polished flat plate. Molten naphthalene is then poured into the molds. After the naphthalene solidifies and the system cools down to room temperature, the molds are separated from the testpiece by applying a shear force. The testpieces are placed and clamped on the measurement table. Initial readings of the naphthalene surface elevation are taken at predetermined locations using the data acquisition system. The testpieces are then installed in the wind tunnel and exposed to the air stream for about 1 h. During a test run, the naphthalene surface temperature, tunnel air temperature and pressure, and free-stream velocity are measured. The testpieces are then removed. A second set of surface elevation measurements is obtained at the same locations as before. Reference points on the metal parts are used to determine the orientation in the measuring system.

The mass transfer coefficient can be determined from

$$h_m = \rho_s \Delta t / \rho_{v,w} \Delta \tau \quad (1)$$

where ρ_s is the density of the solid naphthalene, $\rho_{v,w}$ the naphthalene vapor density on the surface, Δt the net sublimation depth, and $\Delta \tau$ the total exposure time in the wind tunnel. Total naphthalene sublimation depth is calculated from the change in measured surface elevation, and the excess sublimation that accounts for natural convection is subtracted from the total sublimation. During a test run, sublimation depth was generally 0.05–0.20 mm in the two-dimensional flow region, and 0.05–0.45 mm in the three-dimensional flow region. The empirical equation of Ambrose *et al.* [15] is used to determine the naphthalene vapor pressure. From the ideal gas law, naphthalene vapor density on the surface is then evaluated. The results are expressed in terms of the Sherwood number, defined by

$$Sh = h_m d / D \quad (2)$$

where d is the side length of the square cylinder. The mass diffusion coefficient of naphthalene in air, D, is

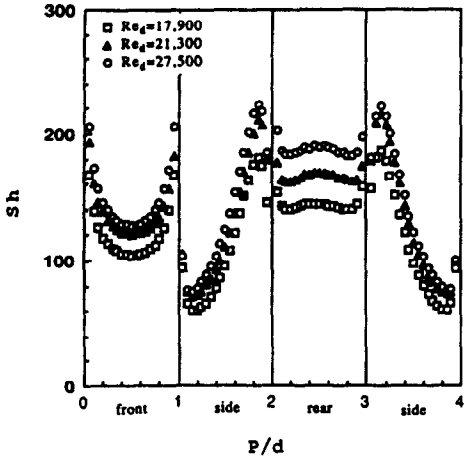

FIG. 2. Local Sherwood number on the square cylinder at various Reynolds numbers in the two-dimensional flow region.

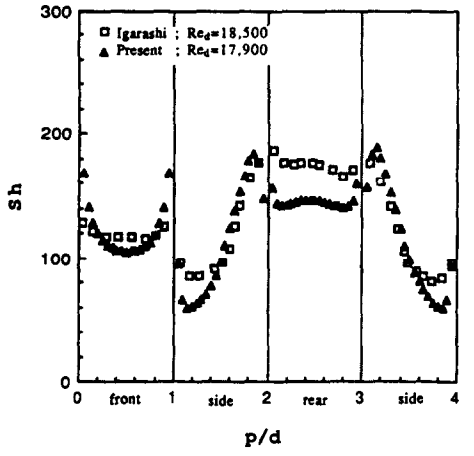

FIG. 3. Comparison of local mass transfer rate on the square cylinder with heat transfer measurements in the two-dimensional flow region.

determined from Mack's measurement data and Chen and Othmer's [16] correlation, which accounts for temperature and pressure variations. Chen [17] reviewed correlations for naphthalene vapor pressure and diffusion coefficient, and recommended Ambrose's equation and Mack's measurement, respectively. The positioning and surface elevation readings using the computer controlled measurement system were found to be very repeatable. Uncertainty analysis according to Kline and McClintock [18] reveals that the estimated errors of the Sherwood numbers are within 6% in the entire range of our measurements.

The oil–lampblack technique is employed to visualize the surface flow on the base plate. Visualization runs are made at the maximum velocity of the air in the wind tunnel, corresponding to Re_d of about 28 000.

RESULTS AND DISCUSSION

Local mass transfer rates on a square cylinder in the two-dimensional flow region were measured and compared with other heat transfer measurements to examine the heat/mass transfer analogy. In addition, detailed mass transfer distributions were obtained both on the square cylinder and on the base plate around the plate–cylinder junction to study the effects of the horseshoe vortex system on the mass transfer process.

Two-dimensional region

Distributions of the Sherwood number on a square cylinder at various Reynolds numbers are shown in Fig. 2. The Sherwood number on the front face increases from the stagnation line to the edges. This trend is in contrast with that of a circular cylinder in which the local transfer rates decrease from stagnation to the separation point. On the side faces, the Sherwood number first decreases in the leading edge separation bubble and then increases thereafter up to the rearward separation corner, which is similar to that seen on a circular cylinder. The Sherwood number on the rear face is almost uniform and higher than that on the front face due to the active turbulent eddy motion in the wake region. Figure 3 presents a comparison of the data with the heat transfer results of Igarashi [4] which were obtained from local temperature measurements using thermocouples under a constant heat flux boundary condition. His data are modified to obtain values of Sh using the heat/mass transfer analogy relation

$$Sh/Nu = [Sc/Pr]^n \tag{3}$$

where the exponent n is taken to be 1/3, as used by Igarashi [4] for the correlation of his data.

Trends in the heat and mass transfer are seen to be very similar to each other except near the trailing edge of the side face, where the mass transfer drops slightly, while the heat transfer coefficient continues to increase. This appears to be related to the fact that, on the rear face, the mass transfer shows much lower convective transport than the heat transfer. One might suspect that the maximum on each side face is due to reattachment. However, other studies [5, 19] do not show any reattachment on the side face of a square cylinder. It is also apparent that the slopes of the mass transfer variation on the front and side face are steeper than found with heat transfer. This implies that mass transfer may be more sensitive to flow change than heat transfer, or the heat transfer results may be affected by wall conduction.

The simple analogy relation, equation (3), should be modified to take into account complex flow conditions. In the recirculation and wake region, for example, turbulent properties such as eddy diffusivity and eddy viscosity play a more important role than the laminar diffusivity and viscosity. Nevertheless, good agreement is found in average transfer rates, as shown in Fig. 4, which indicates that the simple analogy relation is still applicable in an average sense. The

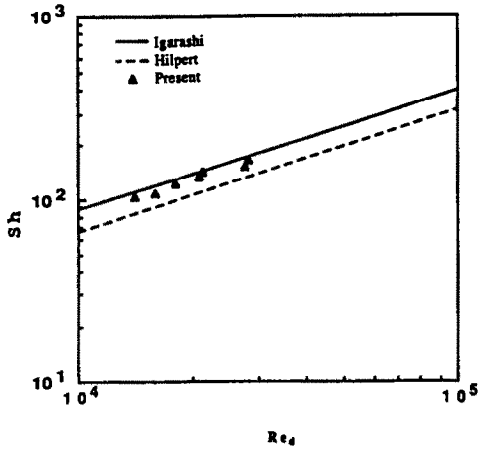

FIG. 4. Comparison of average mass transfer rate on the square cylinder with heat transfer measurements in the two-dimensional flow region.

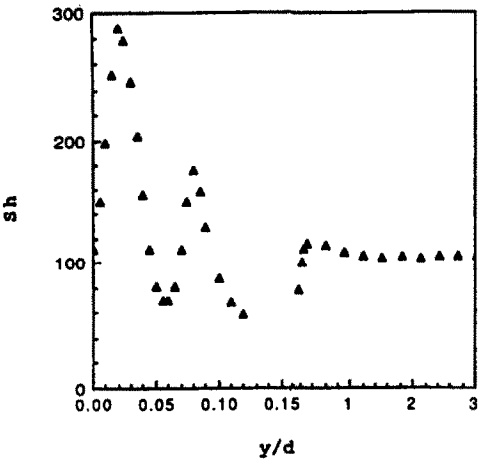

FIG. 6. Distribution of Sherwood number along the front face of the square cylinder at $p/d = 0.5$ ($Re_d = 18\,800$).

present average values are obtained from the summation of local values.

Three-dimensional region

It is well known that a boundary layer flow approaching an obstacle mounted vertically on a flat plate undergoes three-dimensional separation, and that the separated boundary layer rolls up to form a horseshoe vortex system. As many as six vortices, shown in Fig. 5, appear to affect the mass transfer in this study. The size of the primary horseshoe vortex V1 might be expected to be of the same order of magnitude as the freestream boundary layer thickness. The other vortices are an order of magnitude smaller than V1. Many researchers [6, 10, 12–14, 20] found a corner vortex V2, tucked in the plate–cylinder corner. Goldstein and Karni [12] inferred at least one vortex between the primary vortex and corner vortex in interpreting their mass transfer data on a circular cylinder near the base. Considering the rotational direction and mass transfer results, a pair of counterrotating vortices (V3 and V4) seems to be reasonable. Baker [6] and Blair [10] reported the existence of a pair of counterrotating vortices (V5 and V6) beneath the primary vortex upstream of a circular cylinder and a rectangular block, respectively.

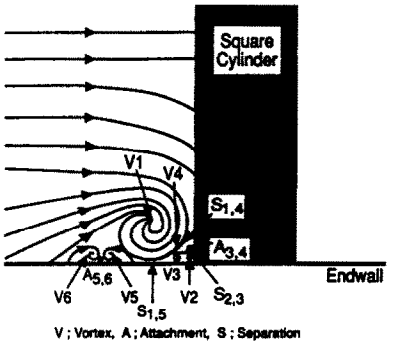

FIG. 5. Schematic of the assumed horseshoe vortex system in the x–y plane at $z = 0$.

Figure 6 presents the distribution of Sherwood number along the front face of the cylinder. Three peaks are found in the figure. The sharp increase very near the base ($y/d \approx 0.02$) is caused by the corner vortex V2. This vortex is so intense that it creates an observable trench in the naphthalene surface during a test run. The peak mass transfer occurs in the down-wash region of a vortex from thinning of the boundary layer. The minimum is associated with the up-wash region, where low momentum fluid from the near-wall zone is swept upward to thicken the boundary layer. Thus the second peak ($y/d \approx 0.08$) is considered to appear in the down-wash region of vortices, indicated by $A_{3,4}$ (attachment of vortices V3 and V4) in Fig. 5. This enhancement diminishes very rapidly. A small enhancement of the mass transfer due to the primary horseshoe vortex is seen at an elevation $y/d \approx 0.3$–1.0. It is interesting to note that the values between the three peaks are lower than the corresponding two-dimensional values. These two minima (at $y/d \approx 0.055$ and 0.12, respectively) apparently correspond to the up-wash region of the vortices, indicated respectively by $S_{2,3}$ (separation of vortices V2 and V3) and $S_{1,4}$ (separation of vortices V1 and V4) in Fig. 5. This trend is very similar to the results in ref. [12] in the front portion of a circular cylinder. The mass transfer at $y/d = 0$, supposed to be zero, is not exactly zero. As shown in Fig. 1, the cylinder is set such that part of its naphthalene covered surface extends from under the base plate, and the flow may penetrate into the gap formed between the cylinder and the adapter of the plate. Careful measurements, in which the solid part of the cylinder was aligned with the upper surface of the plate and the gap was filled with stainless steel foil, revealed that such penetration does not affect the peak positions nor the peak values. Figure 7 shows the contours of Sherwood number on each face of the square cylinder. The side

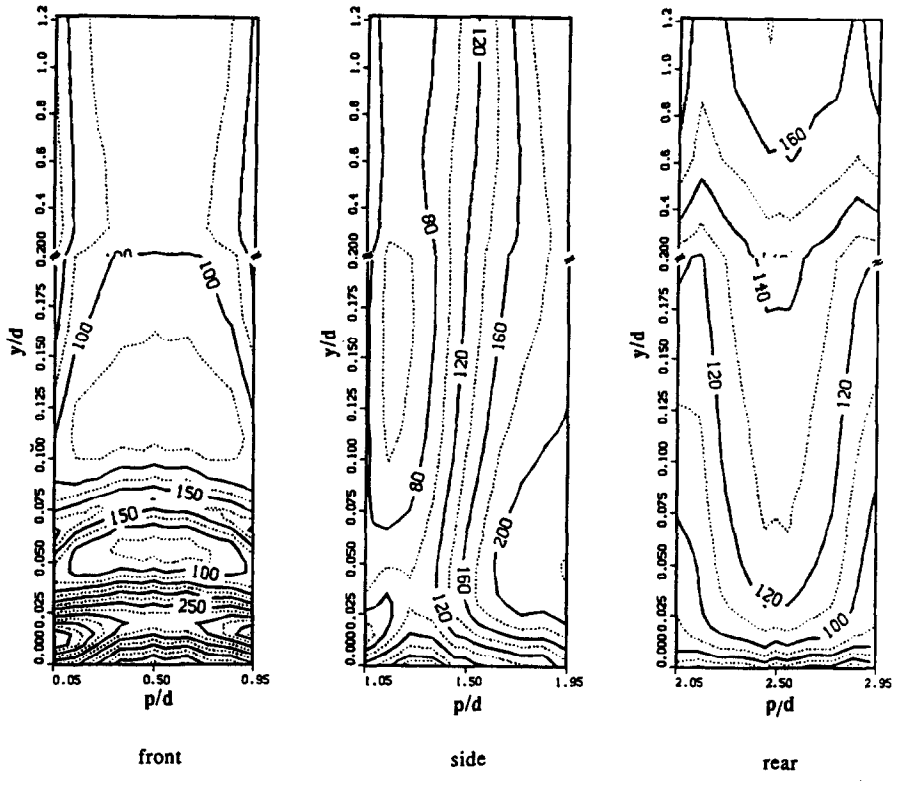

FIG. 7. Contours of Sherwood number on the square cylinder ($Re_d = 18\,800$).

face is slightly influenced by the vortex V2, but there is no evidence of it being affected by other vortices. On the rear face, the Sherwood number increases gradually from zero at the base and asymptotically approaches the two-dimensional values as y increases. The area affected by the base plate extends to a height, y, of about one side length of the cylinder.

The variation of Sherwood number along the streamwise direction on the base plate near the cylinder is shown in Fig. 8. As can be seen from the figure, the corner vortex dramatically augments the mass transfer. The corner vortex V2 formed at the plate–cylinder interface causes a local maximum near the front edge of the cylinder. With separation, it moves away from the side face, and eventually touches the trailing edge of the side face. It finally disappears when interacting with the recirculating flow behind the cylinder. Because of the uncoated part of the adapter, measurements could not be taken very close upstream of the cylinder ($-0.525 < x/d < -0.50$) where extremely high mass transfer rates are expected due to the corner vortex V2. Actually, the closest measurement point was 1.27 mm (0.05 in.) apart from the cylinder. Going upstream from the cylinder, it is interesting to note that a slope change is seen in the region $x/d \approx -0.725$ due to the reattachment of the primary vortex. It is apparent from the figure that this is followed by the local minimum at $x/d \approx -0.9$ and another peak at $x/d \approx -1.05$. This peak is probably too large to be produced by the primary vortex, and may be due to attachment ($A_{5,6}$) of vortices V5 and V6; the minimum is attributed to separation ($S_{1,5}$) of vortices V1 and V5. Similar enhancement has been reported in Blair's [10] heat transfer measurements in the vicinity of a rectangular block. Despite the fact that Baker [6] has observed a pair of counterrotating vortices upstream of a circular cylinder, there is no direct evidence of them in the mass transfer measurements in ref. [13]. These results are in keeping with the observations reported by Ireland and Jones [11]. A significant maximum due to vortex V2 and a weaker

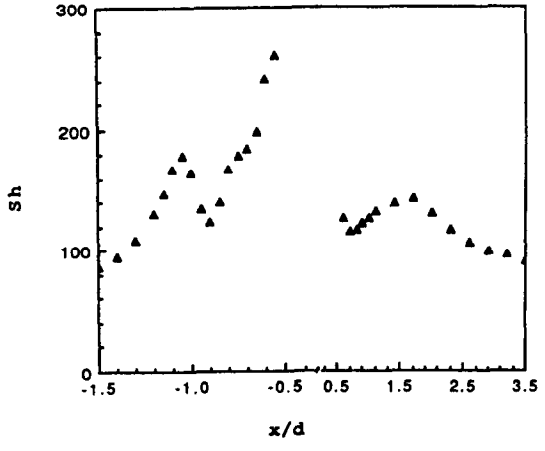

FIG. 8. Distribution of Sherwood number along the streamwise direction on the base plate at $z/d = 0.05$ ($Re_d = 18\,800$).

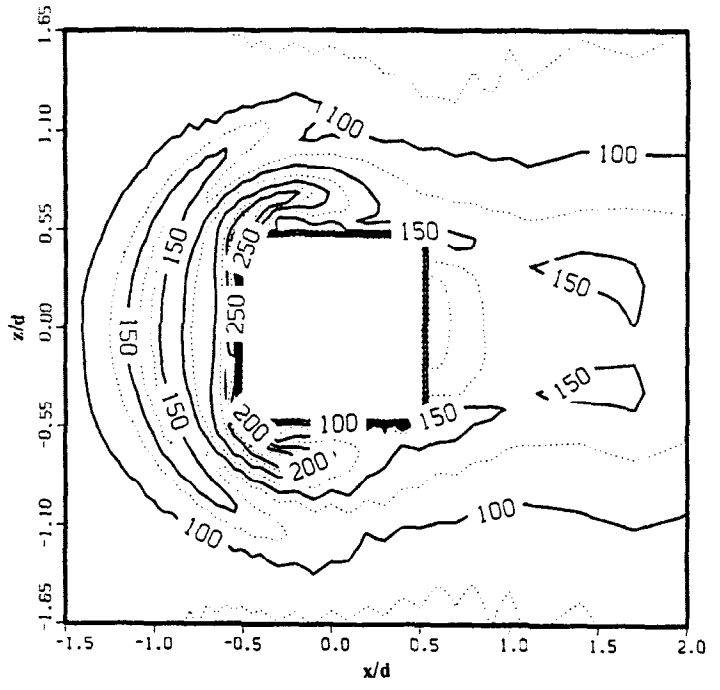

FIG. 9. Contours of Sherwood number on the base plate ($Re_d = 18\,800$).

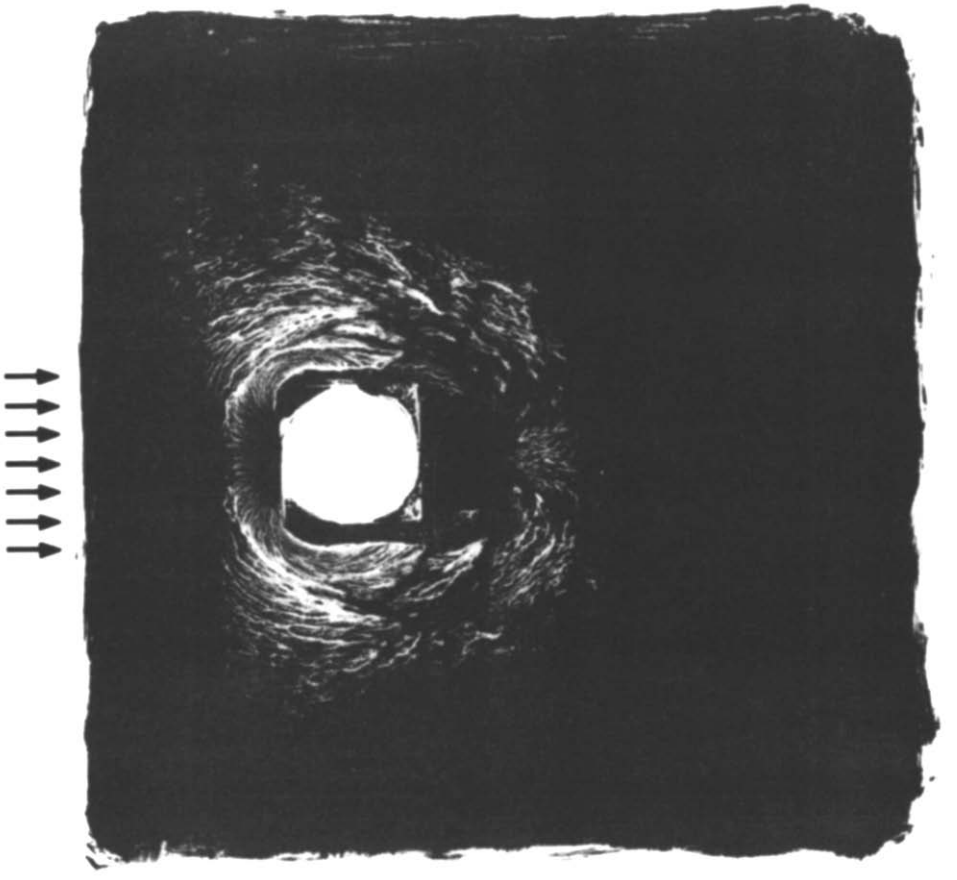

FIG. 10. Visualization of the surface flow on the base plate.

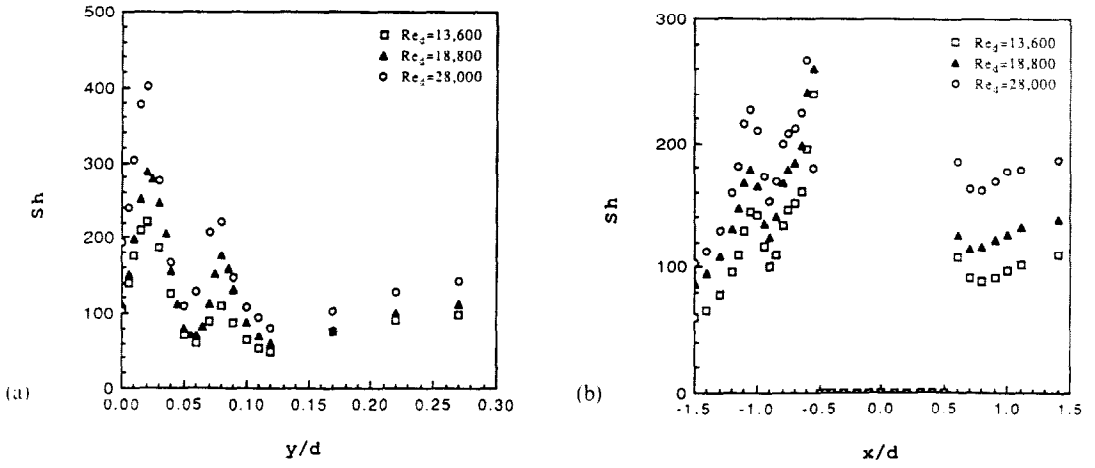

FIG. 11. Variation of Sherwood number on the cylinder and the base plate near the junction for different Reynolds numbers: (a) along the front face of the cylinder ($p/d = 0.5$); (b) along the streamwise direction on the base plate ($z/d = 0.05$).

maximum apparently due to vortex V1 was found while studying a circular cylinder in crossflow [20]. In case of a circular cylinder, counterrotating vortices may not augment the heat or mass transfer on the surface around a protruding cylinder, or influence it only slightly. Contours of Sherwood number on the base plate (Fig. 9) show the trail of peaks created by the counterrotating vortices and the corner vortex. The whole affected area on the base plate extends approximately $1.5d$ upstream, $1.5d$ to the side, and $3d$ downstream from the center of the cylinder location.

The oil–lampblack visualization pattern of the surface flow on the base plate is shown in Fig. 10. The white square area is the site of the cylinder, and the direction of the freestream flow is indicated by the arrows. Horseshoe-like streaks are seen in the figure, which are produced by the primary vortex V1, corner vortex V2, and the pair of counterrotating vortices V5 and V6. Streaks due to the corner vortex and the pair of counterrotating vortices compare quite well, respectively, with the trail of the peaks of Sherwood number created by these vortices in the contour plot.

The influence of the freestream velocity and the boundary layer thickness on mass transfer in the horseshoe vortex system has also been investigated. Figure 11 presents the variation of Sherwood number on the front face of the cylinder and on the base plate at various Reynolds numbers. As the Reynolds number decreases, the mass transfer rates decrease and peaks produced by the vortices appear to diminish. Peaks occur at the same location regardless of the Reynolds number, however. The Reynolds number

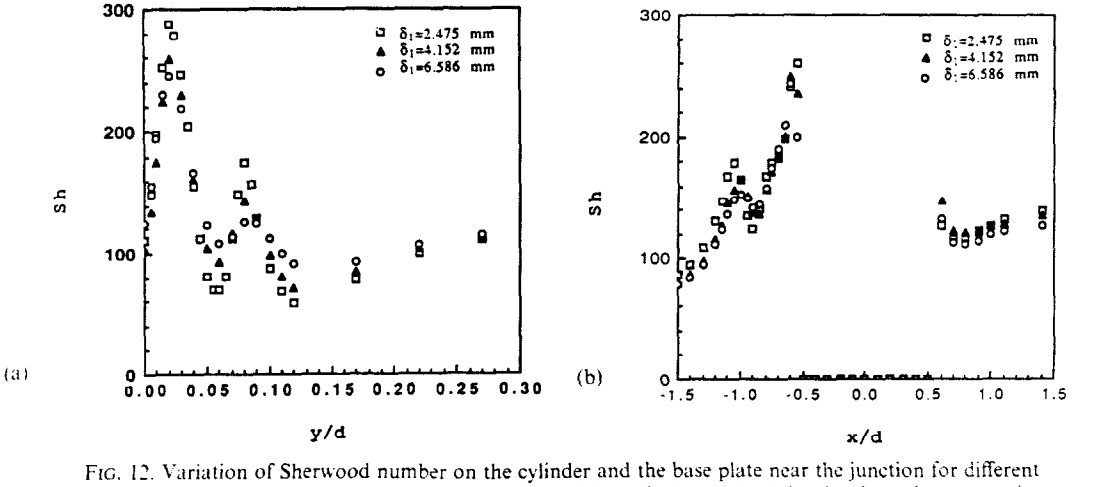

FIG. 12. Variation of Sherwood number on the cylinder and the base plate near the junction for different boundary layer thicknesses: (a) along the front face of the cylinder ($p/d = 0.5$); (b) along the streamwise direction on the base plate ($z/d = 0.05$).

affects the strength of the vortices, but does not change their locations.

Figure 12 shows how the boundary layer thickness affects the mass transfer. Table 1 is given as a supplement to Fig. 12. The thin boundary layer produces a steep spanwise pressure gradient which might be expected to influence the intensity and the size of the vortices. Thickening of the boundary layer might be expected to decrease the peak values and increase the size of the affected region. It can be seen from the figures that an increase in displacement thickness by almost three times does not significantly change the location of the peaks, although their magnitudes are decreased somewhat.

CONCLUSIONS

Detailed measurements of the mass transfer distribution both on the square cylinder in crossflow and its base plate were performed using a naphthalene sublimation technique. A summary of the major results are given below.

(1) The heat/mass transfer analogy equation is valid for comparing average values of transport coefficient, but more insight may be needed when comparing local values in complex turbulent flows.

(2) Multiple vortices, which include the primary horseshoe vortex, the corner vortex and two pairs of counterrotating vortices, affect the mass transfer process in the vicinity of the plate–cylinder junction.

(3) The corner vortex produces extremely high mass transfer both on the cylinder and the base plate. It is so intense that its influence extends even downstream of the cylinder.

(4) Contrary to what has been observed on the base near a circular cylinder in crossflow, a pair of counterrotating vortices beneath the primary vortex is inferred which enhances mass transfer approximately one side length upstream of the center of the cylinder base.

(5) Variation of either Reynolds number or boundary layer thickness does not change the location of peaks created by the horseshoe vortex system. The magnitude of the mass transfer rate strongly depends on the Reynolds number, but it only weakly depends on the initial boundary layer thickness.

REFERENCES

1. H. Reiher, Der wärmeübergang von strömender luft an rohrbündel in kreuzstorm, *VDI ForschHft.* **269**, 47 (1925).
2. R. Hilpert, Wärmeabgabe von geheizten drähten und rohrem in lufstorm, *Gebiete Ingenieurw* **4**, 215–224 (1933).
3. T. Igarashi, Heat transfer from a square prism to an air stream, *Int. J. Heat Mass Transfer* **28**, 175–181 (1985).
4. T. Igarashi, Local heat transfer from a square prism to an air stream, *Int. J. Heat Mass Transfer* **29**, 777–784 (1986).
5. T. Igarashi, Fluid flow and heat transfer around rectangular cylinders (the case of width/height ratio of a section of 0.33–1.5), *Int. J. Heat Mass Transfer* **30**, 893–901 (1987).
6. C. J. Baker, Turbulent horseshoe vortex, *J. Wind Engng Ind. Aero.* **6**, 9–23 (1980).
7. W. A. Eckerle and L. S. Langston, Horseshoe vortex formation around a circular cylinder, *J. Turbomachinery* **109**, 278–285 (1987).
8. P. A. Eibeck and J. K. Eaton, Heat transfer effects of a longitudinal vortex embedded in a turbulent boundary layer, *J. Heat Transfer* **109**, 16–24 (1987).
9. R. A. Graziani, M. F. Blair, J. R. Taylor and R. E. Mayle, An experimental study of endwall and airfoil surface heat transfer in a large scale turbine blade cascade, *J. Engng Pwr* **102**, 257–267 (1980).
10. M. F. Blair, Heat transfer in the vicinity of a large scale obstruction in a turbulent boundary layer, *J. Propulsion* **1**, 158–160 (1985).
11. P. T. Ireland and T. V. Jones, Detailed measurements on heat transfer on and around a pedestal in fully developed passage flow, *Proc. 8th Int. Heat Transfer Conf.*, Vol. 3, pp. 975–980 (1986).
12. R. J. Goldstein and J. Karni, The effect of a wall boundary layer on local mass transfer from a cylinder in crossflow, *J. Heat Transfer* **106**, 260–267 (1984).
13. R. J. Goldstein, M. K. Chyu and R. C. Hain, Measurement of local mass transfer on a surface in the region of the base of a protruding cylinder with a computer controlled data acquisition system, *Int. J. Heat Mass Transfer* **28**, 977–985 (1985).
14. N. Van Dresar and R. E. Mayle, Convection at the base of a cylinder with a horseshoe vortex, *Proc. 8th Int. Heat Transfer Conf.*, Vol. 3, pp. 1121–1126 (1986).
15. D. Ambrose, I. J. Lawrenson and C. H. S. Sparke, The vapor pressure of naphthalene, *J. Chem. Thermodynam.* **7**, 1173–1176 (1975).
16. N. H. Chen and D. F. Othmer, New generalized equation for gas diffusion coefficient, *J. Chem. Engng Data* **7**, 37–41 (1962).
17. P. H. Chen, Measurement of local mass transfer from a gas turbine blade, Ph.D. thesis, University of Minnesota, Minneapolis, Minnesota (1988).
18. S. J. Kline and F. A. McClintock, Describing uncertainty in single-sample experiments, *Mech. Engng* **75**, 3–8 (1953).
19. J. M. Robertson, J. B. Wedding, J. A. Peterka and J. E. Cermak, Wall pressures of separation–reattachment flow on a square prism in uniform flow, *J. Ind. Aero.* **2**, 345–359 (1977/1978).
20. R. J. Goldstein, J. Karni and Y. Zhu, Effect of boundary conditions on mass transfer near the base of a cylinder in crossflow, *J. Heat Transfer*, to be published.

TRANSFERT CONVECTIF DE MASSE A PARTIR D'UN CYLINDRE ET SA PLAQUE DE BASE

Résumé—On étudie le transfert de masse à partir d'un cylindre à section carrée et de la plaque sur laquelle il est monte verticalement, à partir de la technique de la sublimation du naphtalène. La configuration générale du transfert de masse local est sensiblement différent de celle pour un cylindre circulaire. Une comparaison avec d'autres mesures thermiques sur un cylindre carré dans la région d'écoulement bidimensionnel, en utilisant l'analogie chaleur/masse, montre un bon accord dans les flux moyens transférés mais de légères différences dans les valeurs locales. Une grande différence de flux de masse est trouvée à la fois pour le cylindre et la base plane autour de la région de jonction, à cause d'un tourbillon en fer à cheval. La variation du nombre de Reynolds ou bien de l'épaisseur initiale de la couche limite ne change pas significativement la position des pics créés par le système à tourbillon en fer à cheval, mais affecte seulement la valeur du flux local de masse. Une visualisation de l'écoulement sur la base plane est ajoutée aux mesures de transfert de masse.

KONVEKTIVE STOFFÜBERTRAGUNG VON EINEM QUADRATISCHEN ZYLINDER UND SEINER GRUNDPLATTE

Zusammenfassung—Mit der Naphthalin-Sublimationstechnik wird die Stoffübertragung von einem quadratischen Zylinder und seiner Grundplatte untersucht. Die generelle Struktur des lokalen Stofftransports weicht hier etwas von den Verhältnissen am Kreiszylinder ab. Ein Vergleich mit anderen Wärmeübertragungsmessungen an einem quadratischen Zylinder im zweidimensionalen Strömungsbereich zeigt unter Benutzung der Analogie zwischen Wärme- und Stoffübertragung eine gute Übereinstimmung bei Mittelwerten, aber leichte Unterschiede bei lokalen Werten. Der Stoffübergang ändert sich im Bereich der Verbindung von Grundplatte und Zylinder aufgrund eines hufeisenförmigen Wirbelsystems sehr stark. Verschiedene Wirbel, unter anderen der primäre Hufeisen-Wirbel, der Eckwirbel und zwei Paare gegenläufiger Wirbel beeinflussen die Stoffübertragung. Weder eine Variation der Reynolds-Zahl noch die anfängliche Dicke der Grenzschicht bewirken eine signifikante Änderung der Position der Maxima aufgrund des hufeisenförmigen Wirbelsystems, beide beeinflussen lediglich den Betrag des lokalen Stoffübergangs. Ergänzend wurde die Oberflächenströmung an der Grundplatte sichtbar gemacht.

КОНВЕКТИВНЫЙ МАССОПЕРЕНОС ОТ ЦИЛИНДРА КВАДРАТНОГО СЕЧЕНИЯ И ПОДДЕРЖИВАЮЩЕЙ ЕГО ПЛАСТИНЫ

Аннотация—Методом сублимации нафталина исследуется массоперенос от цилиндра квадратного сечения и пластины, на которой он вертикально установлен. Общий режим локального массопереноса несколько отличается от случая с цилиндром круглого сечения. Сравнение с другими измерениями теплопереноса для цилиндра квадратного сечения в области двумерного течения, проведенное при помощи аналогии тепло- и массопереноса, показывает хорошее согласование между средними интенсивностями переноса и небольшие различия между локальными значениями. Как на цилиндре, так и на поддерживающей пластине вокруг области соединения пластины и цилиндра обнаружено резкое изменение интенсивностей массопереноса, вызванное системой подковообразных вихрей. На процесс теплопереноса воздействуют множество вихрей, включающих основной подковообразный вихрь, угловой вихрь и две пары вращающихся в противоположных направлениях вихрей. Изменение числа Рейнольдса или начальной толщины пограничного слоя не приводит к существенному изменению расположений пиков, созданных системой подковообразных вихрей, а влияет лишь на величину скорости локального массопереноса. Дополнительно к измерениям массопереноса проводилась визуализация поверхностного течения на поддерживающей пластине.